

PHYSICAL REVIEW B

CONDENSED MATTER

THIRD SERIES, VOLUME 34, NUMBER 1

1 JULY 1986

Photon-gated spectral hole burning in $\text{LiGa}_5\text{O}_8:\text{Co}^{2+}$

R. M. Macfarlane and J.-C. Vial*

IBM Almaden Research Center, 650 Harry Road, San Jose, California 95120-6099

(Received 3 March 1986)

Photon-gated hole burning, or selective bleaching enabled by a second light source, has been observed in Co^{2+} in tetrahedral sites of LiGa_5O_8 . This leads to long-lived spectral holes with a width of ~ 1 GHz at 1.6 K. It is proposed that two-step photoionization of Co^{2+} is responsible for the hole burning. Much narrower (~ 40 MHz) transient holes and antiholes were burned using population storage in nuclear hyperfine levels. These two mechanisms of hole burning are reported here for transition-metal ions for what is believed to be the first time.

I. INTRODUCTION

Photon-gated spectral hole burning^{1,2} is the selective bleaching of an inhomogeneously broadened absorption by a narrow-band laser, which occurs only in the presence of a second, possibly broad-band gating light source. Gated hole burning can produce long-lived holes which are very stable to probing light—a factor of great importance in applications to high-resolution laser spectroscopy³ and to frequency-domain information storage.⁴ In addition, since this is a new hole-burning mechanism, it extends the applicability of spectral hole burning to new materials as illustrated here by our observation of reversible, photon-gated hole burning in $\text{LiGa}_5\text{O}_8:\text{Co}^{2+}$. This is representative of a new and potentially large class of hole-burning materials containing transition-metal ions of the $3d$, $4d$, or $5d$ series which exhibit multiple valence states and which may show two-photon ionization under suitable conditions.

II. ELECTRONIC STRUCTURE AND SPECTROSCOPY

The unit cell of the ordered inverse spinel LiGa_5O_8 contains four formula units with twelve octahedral and eight tetrahedral Ga^{3+} sites,⁵ which can be substituted by Co^{2+} . The Co^{2+} ions show a preference for tetrahedral sites but can occupy octahedral sites as well.

The flux-grown sample of $\text{LiGa}_5\text{O}_8:\text{Co}^{2+}$ used in these experiments exhibited two zones of concentration: a deep blue core and a pale blue outer region. The color is due to Co^{2+} in tetrahedral sites for which the odd-parity crystal field is large, resulting in an oscillator strength which is typically high for a $d \rightarrow d$ transition ($\approx 10^{-3}$). Electron

beam microprobe measurements of the cobalt concentration gave 0.5% in the dark area and 0.12% in the pale area. The percentage of cobalt ions occupying octahedral sites is not known but is presumed to be smaller than that for tetrahedral sites which dominate the optical absorption and are the only ones that concern us here.

The ground state of tetrahedrally coordinated Co^{2+} is 4A_2 and there are three excited quartet states ${}^4T_2(F)$, ${}^4T_1(F)$, and ${}^4T_1(P)$ (Fig. 1).⁶ In the absence of spin-orbit coupling, only the ${}^4A_2 \rightarrow {}^4T_1$ transitions are allowed, and these dominate the actual absorption spectrum. Our measurements were made at 1.6 K on the ${}^4A_2 \rightarrow {}^4T_1(P)$ transition around 6600 Å (Fig. 2). This has been studied by Donegan⁷ and Donegan *et al.*⁸ who reported the observation of emission from ${}^4T_1(P)$ with a lifetime of 200 nsec at low temperatures. This short lifetime and the strong absorption and emission show that 4T_1 lies below 2E in contrast to the case⁹ of $\text{ZnAl}_2\text{O}_4:\text{Co}^{2+}$. The level diagram of Fig. 1 is approximate, having been taken from Ferguson⁶ using a tetrahedral field parameter $Dq = -240$ cm^{-1} , and Racah parameters $B = 720$ cm^{-1} and $C = 4.6$ B . This differs from the set used by Donegan *et al.*⁸ but it displays the correct qualitative level structure. Our measurements were made on the zero-phonon line at 6600 Å, which has a width of 20 cm^{-1} and contains $\approx 10\%$ of the total intensity of the transition—the remainder being in the phonon sideband. The absorption coefficient integrated over the zero-phonon line and the phonon sideband was 9.9×10^3 cm^{-2} for a section of crystal containing 0.12 at. % cobalt, i.e., $2.5 \times 10^{19}/\text{cm}^3$. From this, we obtain an oscillator strength $f = 5 \times 10^{-4}$. This should be considered a lower limit because the electron-beam microprobe gave total cobalt content rather than the amount of divalent cobalt on tetrahedral sites. This oscillator strength contributes ≈ 1.5 μsec to the radiative decay

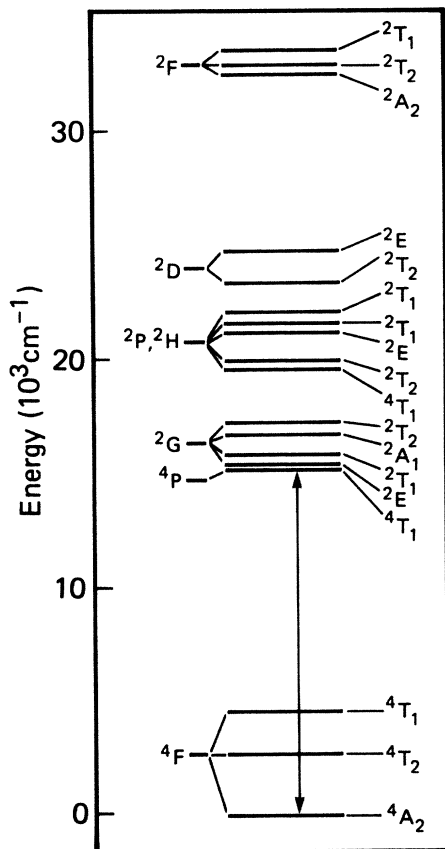


FIG. 1. Energy-level diagram of Co^{2+} in tetrahedral sites for a tetrahedral crystal-field strength $Dq = -240 \text{ cm}^{-1}$ and Racah parameters $B = 720 \text{ cm}^{-1}$ and $C = 3300 \text{ cm}^{-1}$.

time. The radiative branching ${}^4T_1(P) \rightarrow {}^4T_1(F)$, 4T_2 , and 4A_2 is not known but assuming comparable intensities in the three bands, the fluorescence quantum efficiency has the rather large value of 10%. Donegan⁷ also proposes a high quantum efficiency for fluorescence based on the observation that the lifetime is independent of temperature up to about 350 K.

We found that the zero-phonon line showed unresolved structure, and also that the emission and absorption spectra do not coincide exactly in frequency (see Fig. 2 inset). This suggested a splitting of both ground and excited states by several cm^{-1} . While a splitting of the excited state is expected due to spin-orbit coupling, the presence of a ground-state splitting necessarily implies a distortion from T_d symmetry which is not reported in the crystal structure determination.⁵ Other measurements, notably the EPR of Fe^{3+} in the ordered phase of LiAl_5O_8 which is isomorphous with LiGa_5O_8 (Ref. 10) and fluorescence of Fe^{3+} in LiGa_5O_8 (Ref. 11) show evidence of a strong axial distortion in the tetrahedral site. In these cases, unlike that of a Co^{2+} dopant, charge compensation is not required so it appears that the nominally tetrahedral site of LiGa_5O_8 has an intrinsic axial symmetry.

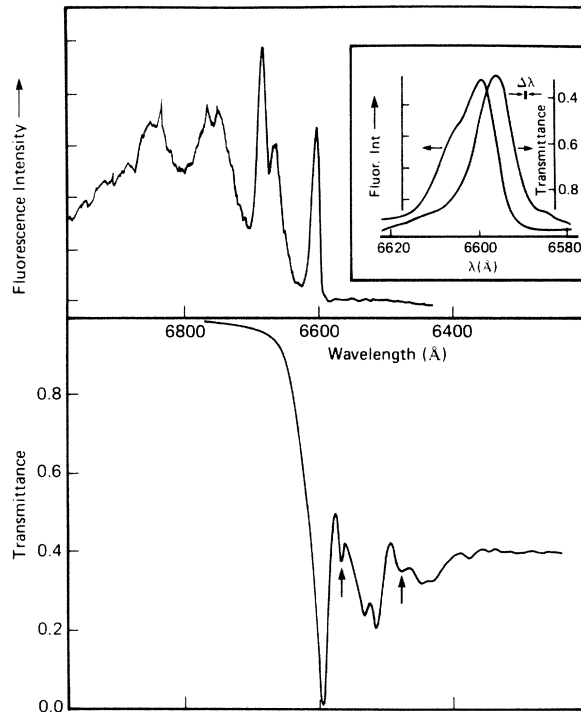


FIG. 2. Transmission and fluorescence spectra of the ${}^4A_2 \leftrightarrow {}^4T_1(P)$ transition of LiGa_5O_8 containing 0.12 at. % Co^{2+} at 1.6 K. The crystal thickness was 1.5 mm. Some absorption features were observed which do not appear in the excitation spectrum of the fluorescence and hence do not arise from Co^{2+} in the tetrahedral site. These have been removed from the transmission spectrum at wavelengths longer than the zero-phonon line. The two absorption peaks marked with arrows are also probably not associated with the center of interest. The inset is a magnification of the zero-phonon line for a 0.28-mm crystal thickness showing the shift between emission and absorption because of splittings in the ground and excited states.

III. PHOTON-GATED HOLE BURNING

Two cw dye lasers were used for gated hole burning. One was a single-frequency laser with a jitter width of ~ 3 MHz (the frequency-selective laser) and the other—the gating laser—was multimode. The beams were combined and incident at 45° on to the face of a $300\text{-}\mu\text{m}$ -thick, polished sample. Fluorescence was collected at 90° to the incident light and detected by a photomultiplier through a filter transmitting beyond 7100 \AA .

Persistent hole burning was observed with a single, resonant narrow-band laser for exposures of ~ 1 sec at $\sim 1 \text{ W/cm}^2$. Probing was done by scanning the laser attenuated by 10^{-2} and monitoring the fluorescence. The width of shallow ($\sim 5\%$) holes was quite large, about 1 GHz, and became larger for deeper holes. In addition, there was a dependence of the hole width and the hole shape on position in the inhomogeneous line profile. On the high-frequency side of the line, where excitation is to

an upper component of 4T_1 the holes are broader (~ 10 GHz). This may result from fast (~ 30 psec) relaxation between ${}^4T_1(2)$ and ${}^4T_1(1)$, for example, but there are no independent measurements to confirm this.

Measurements of the hole area as a function of power at constant energy showed a faster than linear dependence, suggesting a two-step or gated process. This was confirmed by measurements with two lasers—one resonant with the zero-phonon line, and the other tuned to an energy below that of the ${}^4A_2 \rightarrow {}^4T_1(P)$ transition. In a typical experiment, the frequency selective laser power density was reduced to ~ 20 mW/cm² and the gating laser had 10 W/cm². A gating ratio, i.e., the ratio of the areas of gated and ungated holes, of more than 20 was observed (Fig. 3). An action spectrum of gating was not measured but at least wavelengths longer than 6600 Å were effective.

The hole burning was reversible and hole erasure occurred following irradiation with a single laser source over a wide range of wavelengths. The erasure action spectrum in the vicinity of the 6600-Å zero-phonon line followed the Co^{2+} absorption (see Fig. 4). An erasing exposure was

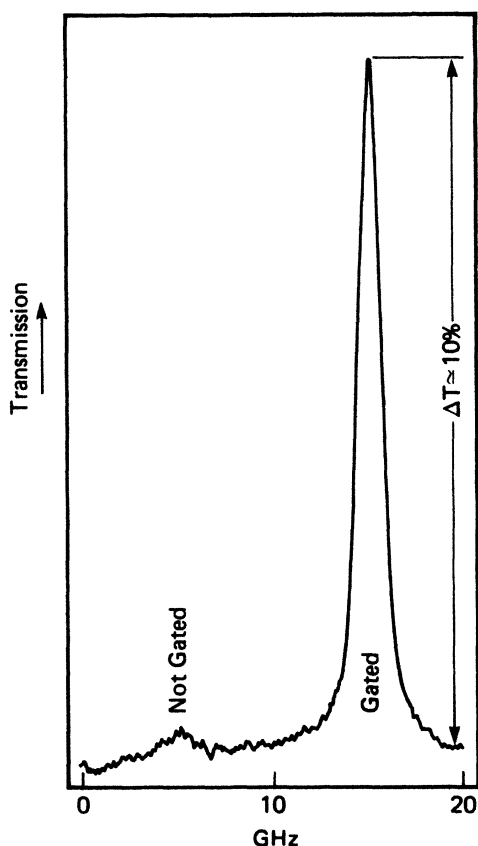


FIG. 3. Illustration of photon-gated hole burning in the 6600-Å zero-phonon line of $\text{LiGa}_5\text{O}_8:\text{Co}^{2+}$. The ungated hole was burned at 6604 Å with 1 W/cm² of cw laser light for 5 sec. For the gated hole, 100 W/cm² of nonresonant 6734-Å light was added and a gating ratio of 21 obtained. The two holes were burned 10 GHz apart for convenience of display. No erasing of the first hole by the gating light was observed.

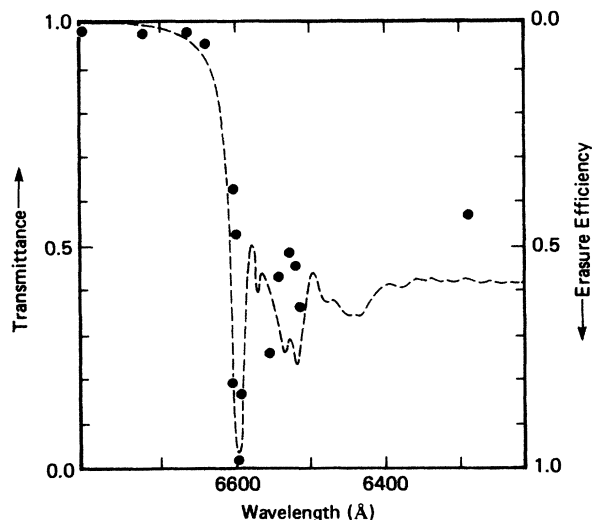


FIG. 4. Erasure efficiency or fractional hole filling under "standard" conditions (see text) as a function of wavelength. The dashed line is the absorption spectrum of Co^{2+} . Wavelengths absorbed by Co^{2+} are effective in erasing, suggesting that a process similar to that of hole burning, i.e., ionization of Co^{2+} in other sites, can produce hole filling.

chosen to produce near complete erasure at the peak of the 6600-Å line, which defined the "standard" erasure conditions. This behavior suggests that at least one mechanism for erasing is photo-oxidation of Co^{2+} and transfer of the electron to the Co^{3+} ions produced by hole burning. Much work is needed to get a complete picture of the mechanisms of hole burning and erasure but we offer the following comments. The photoionized electron released during burning may be trapped at a variety of sites. Co^{3+} present substitutionally on Ga^{3+} sites does not require charge compensation and so would act as a weaker trap than Co^{3+} produced by ionizing a charge-compensated Co^{2+} . Further, the Co^{2+} ions lacking a charge compensator would probably absorb at a different wavelength from the centers studied here. The erasure excitation spectrum may then be due simply to releasing electrons from charge-compensated Co^{2+} incorporated during crystal growth, not those produced by trapping. Eventually, of course, Co^{2+} near charge compensators will be produced by burning and these should be effective traps. The possible role of charge compensators makes this a more complex situation than in $\text{BaClF}:\text{Sm}^{2+}$, for example.¹ We thus have a picture where erasing and gated hole burning can be competitive processes. At wavelengths where Co^{2+} absorbs, the balance favors erasing. Hence, gating wavelengths are chosen where the material is transparent for absorption from the ground state.

The measured hole widths of ~ 1 GHz are much larger than the limit of 0.8 MHz implied by the 200-nsec population decay time, the 1–2 MHz expected for magnetic interactions with Li or Ga nuclear spins, or the frequency jitter contribution of 6 MHz. Measurements with very different absorbed energies showed that laser heating was

not a factor in hole broadening. Further confirmation of this follows from the transient hole burning described below.

IV. TRANSIENT HOLE BURNING

To investigate further the origins of the hole width, transient hole burning was carried out using two narrow-band cw dye lasers. The laser power density in these experiments was 1–10 W/cm². Perhaps surprisingly, much narrower holes (~40 MHz) were observed under these conditions. Similar laser power densities were used as for persistent hole burning. A significant difference between the two experiments, however, is the time scale of the burning process. There are a number of cases now known¹² where long-time-scale persistent hole burning produces hole widths larger than homogeneous linewidths measured on the same transition using different techniques with much shorter time scales. One implication is that slowly time varying local fields, perhaps due to mobile charges, lead to spectral diffusion, but much work remains to clarify this issue. In any event, the holes can be used as very convenient sensitive probes for high-resolution spectroscopy.

Figure 5 shows another interesting property of the transient holes, i.e., the presence of additional holes and antiholes (regions of increased absorption) with separations of 50–100 MHz from the central hole. This pattern is familiar in hole burning due to optical pumping of nuclear hyperfine levels of the rare-earth ions Eu³⁺ and Pr³⁺, for example,¹³ but has not previously been seen in transition metals. Holes correspond to excited-state hyperfine splittings and antiholes to combinations of ground- and excited-state splittings. ⁵⁷Co has a nuclear spin $I = \frac{7}{2}$, which couples to the electron spin of the Kramers doublet in axial symmetry to give eight equally spaced hyperfine levels in first order. The hyperfine constant A of Co²⁺ in LiGa₅O₈ is not known, but in another tetrahedrally coordinated compound ZnO:Co²⁺ $A = 48$ MHz,¹⁴ similar to the splittings observed here. A full analysis of the transient hole spectrum will require rf optical double resonance measurements. Finally, we note that

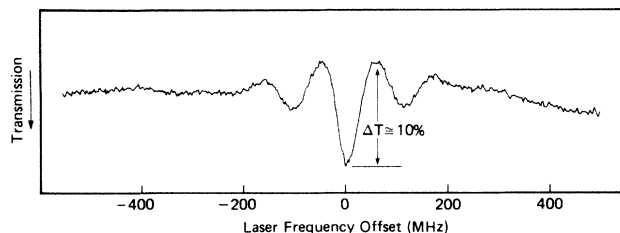


FIG. 5. Hole burning measured with two resonant narrow-band (~MHz) lasers. These holes are transient, in contrast to the persistent gated holes shown in Fig. 5, and are significantly enhanced by the presence of a small external magnetic field of ~300 G, the value used in obtaining the data shown here.

the depth of the transient holes was very dependent on the external magnetic field over the range we used, i.e., 0–200 G. This probably results from a modification of the branching ratios in the optical pumping cycle.

V. CONCLUSION

We have demonstrated clearly that photon-gated spectral hole burning occurs in LiGa₅O₈:Co²⁺. Under our experimental conditions, this leads to persistent holes with an enhancement factor or “gating ratio” of more than 20. The hole widths are anomalously broad but still $\leq \frac{1}{400}$ of the inhomogeneous linewidth. LiGa₅O₈:Co²⁺ is an example of a potentially large class of transition-metal compounds in which gated hole burning may be observed. If such generality is realized, a new and very useful technique of high-resolution laser spectroscopy will develop.

In addition, we have observed transient hole burning due to optical pumping of the Co²⁺ nuclear hyperfine levels. This result, new for transition metals, suggests that the techniques which have been so powerful in the study of rare-earth metals have wider applicability.

ACKNOWLEDGMENTS

We thank Professor G. F. Imbusch for a crystal of LiGa₅O₈:Co²⁺ grown by Dr. J. P. Remeika, and Mr. J. Donegan for a copy of his M.Sc. thesis.

*Permanent address: Laboratoire de Spectrometrie Physique, Université de Grenoble, Boite Postale 87, 38402 Saint Martin d’Hères Cedex, France.

¹A. Winnacker, R. M. Shelby, and R. M. Macfarlane, *Opt. Lett.* **10**, 350 (1985).

²H. W. H. Lee, M. Gehrtz, E. E. Marinero, and W. E. Moerner, *Chem. Phys. Lett.* **118**, 611 (1985).

³R. M. Macfarlane, R. M. Shelby, and A. Winnacker, *Phys. Rev. B* **33**, 4207 (1986).

⁴W. Lenth and W. E. Moerner, *Opt. Commun.* (to be published).

⁵J. C. Joubert, M. Brunel, A. Waintal and A. Dorif, *C. R. Acad. Sci.* **256**, 532 (1963).

⁶J. Ferguson, *J. Chem. Phys.* **39**, 116 (1963).

⁷J. F. Donegan, M.Sc. thesis, University College, Galway, Ireland, 1984.

⁸J. F. Donegan, F. J. Bergin, G. F. Imbusch, and J. P. Remeika, *J. Lumin.* **31-32**, 278 (1984).

⁹J. Ferguson, D. L. Wood, and L. G. vanUitert, *J. Chem. Phys.* **51**, 2904 (1969).

¹⁰V. J. Folen, *J. Appl. Phys.* **33**, 1084 (1962).

¹¹C. McShera, P. J. Colleran, T. J. Glynn, G. F. Imbusch, and J. P. Remeika, *J. Lumin.* **28**, 41 (1983).

¹²R. M. Macfarlane and R. M. Shelby, in *Laser Spectroscopy VI*, edited by H. P. Weber and W. Lüthy (Springer-Verlag, Berlin, 1983), p. 113; R. M. Macfarlane and R. M. Shelby, *Cryst. Lattice Defects Amorph. Mater.* **12**, 417 (1985).

¹³L. E. Erickson, *Phys. Rev. B* **16**, 4731 (1977); R. M. Macfarlane, R. M. Shelby, A. Z. Genack, and D. A. Weitz, *Opt. Lett.* **5**, 462 (1980).

¹⁴T. L. Estle and M. DeWit, *Bull. Am. Phys. Soc.* **6**, 445 (1961).